Eur. Phys. J. A **9**, 473–477 (2000)

THE EUROPEAN PHYSICAL JOURNAL A

Elastic scattering of intermediate-energy weakly bound particles on ^{12}C nuclei

V.P. Mikhailyuk

Institute for Nuclear Research, Kiev 03680, Ukraine

Received: 13 October 1999 / Revised version: 20 November 2000
Communicated by P. Schuck

Abstract. The differential cross-section for elastic scattering of deuterons at 700 MeV, ^{6}Li and ^{6}He at 2.07 GeV nuclei on ^{12}C nucleus is calculated under the assumption of two-cluster (for deuterons and ^{6}Li) and three-cluster (for ^{6}He) structure of incident particle. For ^{6}Li-^{12}C and ^{6}He-^{12}C elastic scattering it is shown that there are quantitative distinctions in the behaviour of the observables calculated in the above approaches.

PACS. 24.10.Ht Optical and diffraction models – 25.45.-z ^{2}H-induced reactions – 25.45.De Elastic and inelastic scattering

1 Introduction

In recent years considerable attention has been given to the interaction of weakly bound particles with nuclei at intermediate energies.Various approaches were used to describe these processes (see, for example, [1–3] and references therein). One of them is the multiple diffraction scattering theory (MDST) [4]. To describe the elastic scattering of nuclei by nuclei on the basis of MDST the summation of multiple scattering series is usually executed, *i.e.* it is supposed that projectile and target nucleons interact with each other. Unfortunately, elastic scattering of light nuclei on nuclei in the energy region $E \sim 100$ MeV/nucleon cannot be satisfactorily described in the multiple scattering theory with "elementary" free amplitudes [5,6]. In other words, complex nuclei change their properties at the collisions due to the effects of nucleon matter, where they are placed, and the effects of polarizability and "free" amplitudes should be changed to effective [7,8].

At present due to discovery of neutron "halo" in some light nuclei (^{6}He, ^{11}Li etc.) their structure pecularities are intensively investigated (see for example [9–11] and references therein). The recent works on these nuclei based on three-cluster model ($\alpha + \mathrm{n} + \mathrm{n}$ for ^{6}He and $^9\mathrm{Li} + \mathrm{n} + \mathrm{n}$ for ^{11}Li nuclei). From this point of view the ^{6}He nucleus is a more ideal system than ^{11}Li, because the α-core is more inert than the ^{9}Li-core *i.e.* α-core can be really considered as an inert one, while the ^{9}Li nucleus has a pronounced three-cluster structure. Notice that, in spite of this, the theoretical calculations [10,11] show that the dineutron-like configuration and the cigar-like configuration coexist in the ^{6}He nuclei with almost an equal probability. Therefore it is of interest to investigate the manifestation of these two configurations in the scattering of ^{6}He nucleus on ^{12}C nuclei, where the α-cluster structures are sufficiently reliably established.

In this paper the model proposed in [12,13] was developed for the case of deuterons, ^{6}Li and ^{6}He nuclei scattered on ^{12}C nuclei. In sect. 2 the elastic d-^{12}C and ^{6}Li-^{12}C scattering was considered under the assumption of a two-cluster structure of the projectile (n + p for deuterons and α + d for ^{6}Li), and in sect. 3 the ^{6}He-^{12}C scattering was considered under the assumption of a three-cluster structure of the projectile ($\alpha + \mathrm{n} + \mathrm{n}$).

2 Scattering of deuterons and ^{6}Li nucleus on ^{12}C nuclei

In ^{12}C nuclei the α-cluster structure is strongly manifested in their interaction with intermediate-energy particles. By means of the α-cluster model with dispersion and MDST we have described observables in elastic and inelastic scattering of intermediate-energy protons, antiprotons, deuterons and others particles on ^{12}C nuclei [7,8,14]. The results of the calculations were in agreement with the experimental data. We show that taking into account four nucleon correlations of the α-cluster type and the correlations between α-clusters allowed us to obtain a better agreement with the experimental data as compared with the free-nucleon model [14]. Moreover, in this cases the spin-rotation functions differ qualitatively.

According to the α-cluster model with dispersion the carbon nucleus is considered as made up of three α-clusters arranged at the vertices of an equilateral triangle.

Table 1.

E (GeV)	Reaction	β_{c1} (fm^2)	G_{c1} (fm^2)	β_{s1} (fm^2)	G_{s1} (fm^3)
1.37	α-α	$0.691 + i0.194$	$-0.229 + i2.444$		
0.7	d-α	$0.679 + i0.183$	$-0.471 + i1.586$	$0.328 - i0.049$	$-0.469 + i0.215$
0.35	p-α	$0.309 - i0.116$	$-0.092 + i0.857$	$0.498 + i0.098$	$0.206 + i0.397$

These α-clusters can be displaced from their most probable positions of equilibrium. The density of the ^{12}C nuclei is determined by [15]

$$\rho_{\Delta}(\boldsymbol{\xi},\boldsymbol{\eta}) = \int d^3\xi' d^3\eta' \rho_0(\boldsymbol{\xi}',\boldsymbol{\eta}')\Phi_{\Delta}(\boldsymbol{\xi}-\boldsymbol{\xi}',\boldsymbol{\eta}-\boldsymbol{\eta}')\,, \quad (1)$$

$$\rho_0(\boldsymbol{\xi},\boldsymbol{\eta}) = \frac{1}{4\sqrt{3}\pi^2 d^2}\delta(\xi-d)\delta\left(\eta-\frac{\sqrt{3}}{2}d\right)\delta(\boldsymbol{\xi\eta})\,, \quad (2)$$

$$\Phi_{\Delta}(\xi,\eta) = \frac{1}{(\sqrt{3}\pi\Delta^2)^3}\exp\left(-\frac{\xi^2+\frac{4}{3}\eta^2}{2\Delta^2}\right)\,, \quad (3)$$

where $\boldsymbol{\xi}$ and $\boldsymbol{\eta}$ are the Jacobi coordinates of the α -clusters. Parameters d and Δ characterize the distance between α-clusters and the probability of the α-clusters displacement from its most probable position at the vertex of the equilateral triangle, respectively. The values of the parameters d and Δ obtained in [15] allow us to describe the measured form factor of ^{12}C nucleus up to the values of transferred momenta $q \le 3$ fm^{-1}.

According to the MDST, the elastic scattering amplitude of "elementary" particles on ^{12}C nuclei can be determined as

$$f(\mathbf{q}) = \frac{ik}{2\pi}\int d^2b d^3\xi d^3\eta e^{i\mathbf{qb}}\rho_{\Delta}(\boldsymbol{\xi\eta})\Omega(\mathbf{b},\mathbf{r}_j), \quad (4)$$

where $\mathbf{b}$ is the impact parameter, $\mathbf{r}_j$ are the α-cluster coordinates of the ^{12}C nucleus, $\mathbf{q}$ is the transferred momentum, k is the wave vector of the incident particle.

In this formula the profile function $\Omega(\mathbf{b},\mathbf{r}_j)$ is

$$\Omega(\mathbf{b},\mathbf{r}_j) = 1-\prod_{j=1}^{3}[1-\frac{1}{2\pi ik}\int d^2q e^{-i\mathbf{q}(\mathbf{b}-\mathbf{r}_j)}\tilde{f}(\mathbf{q})], \quad (5)$$

where $\tilde{f}(\mathbf{q})$ is the elastic scattering amplitude of the incident particle on the α-clusters of the ^{12}C nucleus. The amplitude $\tilde{f}(\mathbf{q})$ has the form

$$\tilde{f}(\mathbf{q}) = f_c(q) + f_s(q)\boldsymbol{\sigma}\mathbf{n}\,, \quad (6)$$

where $\boldsymbol{\sigma}$ is the spin operator of an incident particle, $n = [k,k']/|[k,k']|$, k and k' are the wave vectors of the incident and scattered particle. In this formula the central $f_c(q)$ and spin-orbit $f_s(q)$ part of the amplitude $\tilde{f}(\mathbf{q})$ can be approximated as follows [14]:

$$f_c(q) = k\sum_{i=1}^{2} G_{ci}\exp(-\beta_{ci}q^2), \quad (7)$$

$$f_s(q) = kq\sum_{i=1}^{2} G_{si}\exp(-\beta_{si}q^2)\,. \quad (8)$$

The parameters G_{c1}, β_{c1}, G_{s1} and β_{s1} are the fitting ones, and parameters G_{c2}, β_{c2}, G_{s2} and β_{s2} are related with G_{c1}, β_{c1}, G_{s1} and β_{s1} through [14]

$$G_{c2} = \frac{3iG_{c1}^2}{32\beta_{c1}}, \qquad \beta_{c2} = \frac{1}{2}\beta_{c1}\,, \quad (9)$$

$$G_{s2} = \frac{3iG_{c1}G_{s1}\beta_{c1}}{8(\beta_{c1}+\beta_{s1})^2}, \qquad \beta_{s2} = \frac{\beta_{c1}\beta_{s1}}{\beta_{c1}+\beta_{s1}}\,. \quad (10)$$

The values of the parameters G_{c1}, β_{c1}, G_{s1} and β_{s1} obtained in [7,8,14] are presented in table 1.

Consider the elastic scattering of deuterons and ^{6}Li nucleus on ^{12}C nuclei. Assuming that deuterons and ^{6}Li nucleus consist of two clusters (n+p configuration for deuterons and α+d for ^{6}Li), we construct the incident particle-target amplitude of the scattering amplitude of their clusters on the ^{12}C nucleus (formulae (4)-(10)). According to [12,13] the elastic scattering amplitude of the two-cluster nucleus by the ^{12}C nucleus can be presented in the form

$$F(\mathbf{q}) = \frac{k}{k_1}f_1(\mathbf{q})S(\gamma_1\mathbf{q}) + \frac{k}{k_2}f_2(\mathbf{q})S(\gamma_2\mathbf{q})$$
$$+\frac{ik}{2\pi k_1 k_2}\int d^2q' f_1(\gamma_2\mathbf{q}+\mathbf{q}')f_2(\gamma_1\mathbf{q}-\mathbf{q}')S(\mathbf{q}'), \quad (11)$$

where $\gamma_i = \frac{m_i}{(m_i+m_j)}$, m_i are the incident particle cluster mass, $i,j = 1,2$.

The structure form-factor $S(q)$ has the form

$$S(q) = \int d^3r|\varphi_0(r)|^2 e^{-i\mathbf{qs}}, \quad (12)$$

where $\varphi_0(r)$ is the wave function of the incident particle.

We have chosen the wave function $\varphi_0(r)$ in the form

$$\varphi_0(r) = \frac{\sqrt{2\alpha\beta(\alpha+\beta)}}{r\sqrt{4\pi}(\alpha-\beta)}[e^{-\alpha r}-e^{-\beta r}], \quad (13)$$

where $\alpha = 0.2314$ fm^{-1} for deuteron and $\alpha = 0.305$ fm^{-1} for ^{6}Li nucleus, $\beta = 5.18\alpha$.

On the basis of the above approach we have calculated the differential cross-section $d\sigma/d\Omega$ (mb/sr) for elastic scattering of deuterons at 700 MeV and of the ^{6}Li nucleus

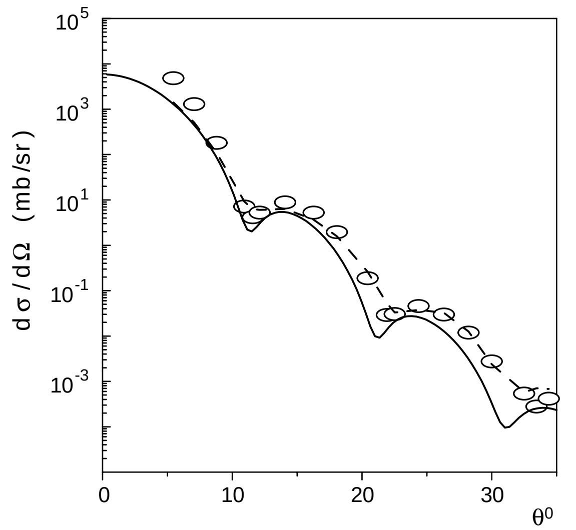

Fig. 1. Differential cross-section of the elastic d-^{12}C scattering at 700 MeV as a function of the scattering angle. Experimental data are from [16].

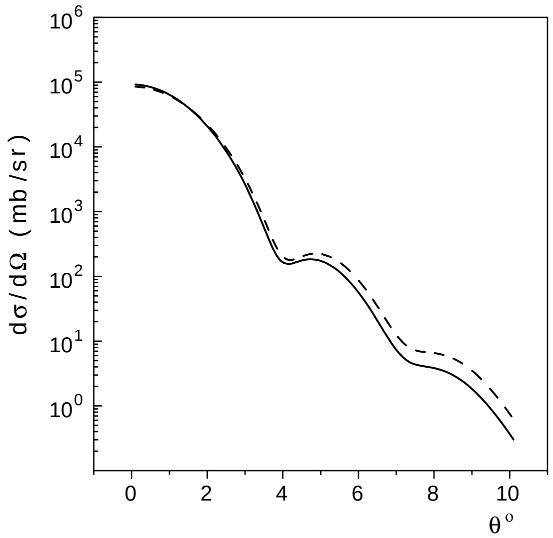

Fig. 2. Differential cross-section of the elastic ^{6}Li-^{12}C scattering at 2.07 GeV as a function of the scattering angle.

at 2.07 GeV on the ^{12}C nucleus. The results obtained are presented in figs. 1 and 2 (solid curves).

As can be seen from fig. 1 the above approach allows us to describe the experimental data without fitting parameters. The dashed curve in fig. 1 presents the results of the calculations where the incident deuteron is considered as an "elementary" particle [7]. The effective d-α amplitude used in this approach automatically includes the effects related with the changing of deuteron structure properties during the interaction with α-clusters of ^{12}C nuclei and the effects of nucleon matter, where the deuteron is placed. As can be seen from fig. 1 the differential cross-section calculated in [7] is in better agreement with experimental data than that calculated in the above approach. We suppose that the discrepancy between the calculated and measured observables can be due to the fact that in the calculations these effects are not properly taken into account. Notice that the small correction to the structure form-factor (12) leads to an improvement in the agreement between the calculated and measured cross-sections.

The dashed curve on fig. 2 has been calculated in the above approach by using the ^{6}Li ground state wave function in the form

$$\psi_1 = \sqrt{\frac{\alpha}{2\pi}}\frac{e^{-\alpha r}}{r}\,. \tag{14}$$

As can be seen from fig. 2 the differential cross-sections for the elastic ^{6}Li-^{12}C interaction calculated with ^{6}Li ground state wave functions in the form (13) and (14) do not differ significantly.

3 Scattering of the ^{6}He nucleus on ^{12}C nuclei

Consider the elastic scattering of the ^{6}He nucleus on ^{12}C nuclei. Assuming that the ^{6}He nucleus has a three-cluster configuration (α + n + n), the elastic scattering ^{6}He-^{12}C amplitude can be presented in the form

$$F(\mathbf{q}) = \frac{ik}{2\pi}\int \mathrm{d}^2b\mathrm{d}^3r\mathrm{d}^3\rho e^{i\mathbf{qb}}|\Psi(r,\rho)|^2$$
$$\times(\omega(\mathbf{b}_1)+\omega(\mathbf{b}_2)+\omega(\mathbf{b}_3)-\omega(\mathbf{b}_1)\omega(\mathbf{b}_2)-\omega(\mathbf{b}_1)\omega(\mathbf{b}_3)$$
$$-\omega(\mathbf{b}_2)\omega(\mathbf{b}_3)+\omega(\mathbf{b}_1)\omega(\mathbf{b}_2)\omega(\mathbf{b}_3))\,, \tag{15}$$

$$\omega(\mathbf{b}_j) = \frac{1}{2\pi ik}\int \mathrm{d}^2qe^{-i\mathbf{qb}_j}f(\mathbf{q}), \tag{16}$$

$$\Psi(r,\rho) = \psi_1(r)\sqrt{\frac{\mu}{2\pi}}\frac{e^{-\mu\rho}}{\rho}\,, \tag{17}$$

where $\boldsymbol{\rho} = \mathbf{r}_\alpha - \frac{1}{2}(\mathbf{r}_{n1}+\mathbf{r}_{n2})$, $\mathbf{r} = \mathbf{r}_{n1}-\mathbf{r}_{n2}$ are the Jacobi coordinates of ^{6}He clusters, the amplitude $f(\mathbf{q})$ is given by eqs. (4)–(10), α=0.429 fm^{-1}, μ=0.136 fm^{-1}.

Integrating (15) we have

$$F(\mathbf{q}) = F_1(\mathbf{q})+2F_2(\mathbf{q})+2F_3(\mathbf{q})+F_4(\mathbf{q})+F_5(\mathbf{q}), \tag{18}$$

$$F_1(\mathbf{q}) = \frac{k}{k_1}f_1(\mathbf{q})S_1(\mathbf{q}), \tag{19}$$

$$F_2(\mathbf{q}) = \frac{k}{k_2}f_2(\mathbf{q})S_2(\mathbf{q}), \tag{20}$$

$$F_3(\mathbf{q}) = \frac{ik}{2\pi k_1k_2}\int \mathrm{d}^2q'f_1(\mathbf{q}')f_2(\mathbf{q}-\mathbf{q}')S_3(\mathbf{q},\mathbf{q}'), \tag{21}$$

$$F_4(\mathbf{q}) = \frac{ik}{2\pi k_2k_3}\int \mathrm{d}^2q'f_2(\mathbf{q}')f_3(\mathbf{q}-\mathbf{q}')S_4(\mathbf{q},\mathbf{q}'), \tag{22}$$

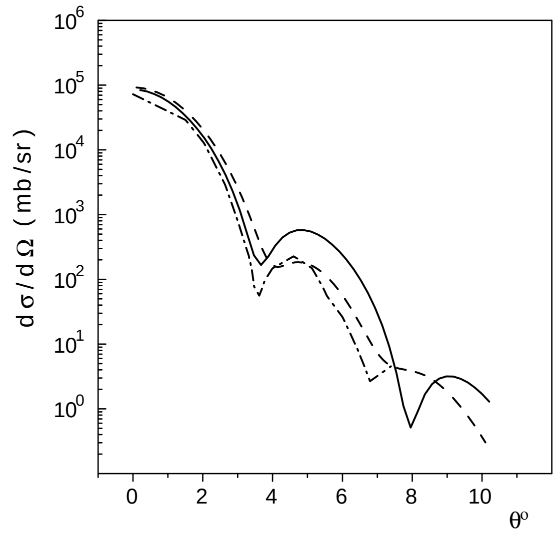

Fig. 3. Differential cross-section of the elastic ^{6}He-^{12}C scattering at 2.07 GeV as a function of the scattering angle.

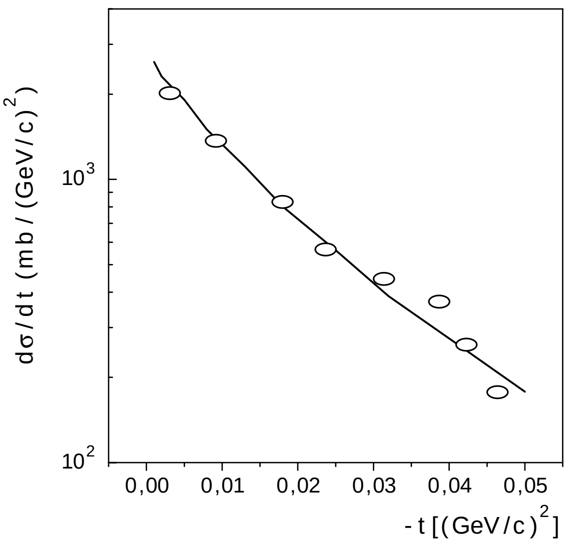

Fig. 4. Differential cross-section of the elastic p-^{6}He scattering at 717 MeV as a function of the momentum transferred. Experimental data are from [17].

$$F_5(\mathbf{q}) = \frac{ik}{(2\pi)^2 k_1 k_2 k_3} \int \mathrm{d}^2 q' d^2 q'' f_1(\mathbf{q} - \mathbf{q}' - \mathbf{q}'') \times f_2(\mathbf{q}') f_3(\mathbf{q}'') S_5(\mathbf{q}, \mathbf{q}', \mathbf{q}''), \quad (23)$$

$$S_1(q) = \int \mathrm{d}^3 r \mathrm{d}^3 \rho |\Psi(r,\rho)|^2 e^{-i2\beta_2 \mathbf{qw}}, \quad (24)$$

$$S_2(q) = \int \mathrm{d}^3 r \mathrm{d}^3 \rho |\Psi(r,\rho)|^2 e^{-i\mathbf{a_1 q}}, \quad (25)$$

$$S_3(q) = \int \mathrm{d}^3 r \mathrm{d}^3 \rho |\Psi(r,\rho)|^2 e^{-i\mathbf{a_1 q} - i\mathbf{a_2 q}'}, \quad (26)$$

$$S_4(q) = \int \mathrm{d}^3 r \mathrm{d}^3 \rho |\Psi(r,\rho)|^2 e^{-i\mathbf{a_1 q} + i\mathbf{q}'\mathbf{s}}, \quad (27)$$

$$S_5(q) = \int \mathrm{d}^3 r \mathrm{d}^3 \rho |\Psi(r,\rho)|^2 e^{-i2\beta_2 \mathbf{qw} + i\mathbf{a_3 q}' + i\mathbf{a_4 q}''}, \quad (28)$$

where $\mathbf{a}_1 = -\beta_1 \mathbf{w} + \frac{1}{2}\mathbf{s}$, $\mathbf{a}_2 = \mathbf{w} + \mathbf{s}$, $\mathbf{a}_{3,4} = \mathbf{w} \mp \frac{1}{2}\mathbf{s}$, $\mathbf{w}$ and $\mathbf{s}$ are the projections of the vectors $\boldsymbol{\rho}$ and $\mathbf{r}$ on the plane perpendicular to the incident ^{6}He direction.

On the basis of the above approach we have calculated the differential cross-section $\mathrm{d}\sigma/\mathrm{d}\Omega$ (mb/sr) for the elastic scattering of the ^{6}He nucleus at 2.07 GeV on ^{12}C nucleus. The results obtained are presented in fig. 3 (solid curve). The dashed curve in fig. 3 is calculated in sect. 2 for elastic ^{6}Li-^{12}C scattering at 2.07 GeV (fig. 2, the dashed curve). The dot-dashed curve was calculated in [3] by means of direct evaluation of Glauber integrals using the Monte Carlo method.

Notice that the ^{6}He wave function used allows us to describe the differential cross-section of the elastic p-^{6}He scattering at 717 MeV (fig. 4, solid curve). The calculations have been executed by means of MDST with the p-α amplitude from [14] and the p-n amplitude from [18].

As can be seen from fig. 3 in the region of the second and third maxima there are quantitative distinctions in the behaviour of the observables calculated in these approaches. These distinctions can be due to manifestation of three and two cluster configurations in ^{6}He and ^{6}Li nuclei. In other words, in the above approach ^{6}He and ^{6}Li nuclei differ only by configuration choice (the three-cluster one for the ^{6}He nucleus and the two-cluster one for the ^{6}Li nucleus). In the approach we have neglected the Coulomb interaction. At the energy considered the Coulomb interaction can give a contribution in the region of the first maxima, since there distinctions between the calculated observables are small. Therefore, we suppose that the distinctions in the calculated differential cross-sections are due to manifestation of the two- and three-cluster configuration mode in ^{6}He and ^{6}Li nuclei. Unfortunately, the lack of experimental data on the ^{6}He,^{6}Li-^{12}C scattering at 2.07 GeV does not allow us to reconstruct the ^{6}He,^{6}Li-^{12}C elastic scattering amplitude with reasonable precision. The experimental investigation of these processes can give the information needed.

The author is indebted to Prof. Yu.A. Berezhnoy, Dr. V.V. Pilipenko and Dr. Yu.A. Pozdnyakov for valuable discussions.

References

1. M.S. Hussein, G.R. Satchler, Nucl. Phys. A **567**, 97 (1994).
2. D.R. Sarker, Md.A. Rahmnan, M. Rahmnan, H.M. Sen-Gupta, Nuovo Cimento A **107**, 511 (1994).
3. F.A. Gareev, S.N. Ershov, G.S. Kazasha, S.Yu. Shmakov, V.V. Uzshinsky, Sov. J. Nucl. Phys. **58**, 620 (1995).
4. R.J. Glauber, in: *Lectures in Theoretical Physics* edited by W.E. Brittin, L.G. Dunham (Interscience, New York, 1959). Vol. 1, p. 315.

5. M.E. Brandan, H. Chehime, K.W. McVoy, Phys. Rev. C **55**, 1353 (1997).
6. M.E. Brandan, K.W. McVoy, Phys. Rev. C **55**, 1361 (1997).
7. V.P. Mikhailyuk, Mod. Phys. Lett. A **10**, 2915 (1995).
8. Yu.A. Berezhnoy, V.P. Mikhailyuk, Z. Phys. A **355**, 1 (1996).
9. K. Varga, Y. Suzuki, R.G. Lovas, Nucl. Phys. A **571**, 447 (1994).
10. S. Funada, H. Kameyama, Y. Sakuragi, Nucl. Phys. A **575**, 93 (1994).
11. V.P. Verbitsky, Yu.A. Pozdnyakov, K.O. Terenetsky, Izvestia Rosijskoi Akademij Nauk **60**, 52 (1996).
12. A.G. Sitenko, E. Ismatov, V.K. Tartakovsky, Sov. J. Nucl. Phys. **5**, 573 (1967).
13. Yu.A. Berezhnoy, A.P. Soznik, Ukr. Phys. J. **18**, 29 (1973).
14. Yu.A. Berezhnoy, V.P. Mikhailyuk, V.V. Pilipenko, J. Phys. G **18**, 85 (1992).
15. Yu.A. Berezhnoy, V.V. Pilipenko, G.A. Khomenko, J. Phys. G **10**, 63 (1984).
16. R. Bertey, L. Bimbot, A. Bondart, J.L. Escudié, J.M. Fountaine, A. Chaumaux, P. Couvert, L. Shecter, J.P. Tabet, Y. Terrien, CEN Saclay, Departement de Physique Nucleaire, Compte rendue d'activité: 110 (1976–1977)
17. S.R. Neumaler, G.D. Alkhazov, M.N. Andronenko et al., *The Fourth International Conference on Radioactive Nuclear Beams, Omiya, Japan* (1996) p. 135.
18. J.A. McNeil, L. Ray, S.J. Wallace, Phys. Rev. C **27**, 2123 (1983).